HHS Public Access
Author manuscript
Cancer Res. Author manuscript; available in PMC 2018 August 15.

Published in final edited form as:
Cancer Res. 2017 August 15; 77(16): 4258–4267. doi:10.1158/0008-5472.CAN-17-1052.

Unpaired Extracellular Cysteine Mutations of CSF3R Mediate Gain or Loss of Function

Haijiao Zhang[1], **Sophie Means**[1], **Anna Reister Schultz**[1], **Kevin Watanabe-Smith**[1], **Bruno C. Medeiros**[2], **Daniel Bottomly**[3], **Beth Wilmot**[3], **Shannon K. McWeeney**[3], **Tim Kükenshöner**[4], **Oliver Hantschel**[4], and **Jeffrey W. Tyner**[1]

[1]Department of Cell, Developmental & Cancer Biology, Oregon Health & Science University Knight Cancer Institute, Portland, Oregon [2]Department of Medicine, Stanford University School of Medicine, Stanford, California [3]Division of Bioinformatics and Computational Biology, Department of Medical Informatics and Clinical Epidemiology, Oregon Health & Science University Knight Cancer Institute, Portland, Oregon [4]Swiss Institute for Experimental Cancer Research (ISREC), School of Life Sciences, École Polytechnique Fédérale de Lausanne (EPFL), Lausanne, Switzerland

Abstract

Exclusive of membrane-proximal mutations seen commonly in chronic neutrophilic leukemia (e.g., T618I), functionally defective mutations in the extracellular domain of the G-CSF receptor (CSF3R) have been reported only in severe congenital and idiopathic neutropenia patients. Here, we describe the first activating mutation in the fibronectin-like type III domain of the extracellular region of CSF3R (W341C) in a leukemia patient. This mutation transformed cells via cysteine-mediated intermolecular disulfide bonds, leading to receptor dimerization. Interestingly, a CSF3R cytoplasmic truncation mutation (W791X) found on the same allele as the extracellular mutation and the expansion of the compound mutation was associated with increased leukocytosis and disease progression of the patient. Notably, the primary patient sample and cells transformed by W341C and W341C/W791X exhibited sensitivity to JAK inhibitors. We further showed that

Corresponding Author: Jeffrey W. Tyner, Oregon Health and Science University, 3181 SW Sam Jackson Park Road, Mailcode L592, Portland, OR 97239. Phone: 503-346-0603; Fax: 503-494-3688; tynerj@ohsu.edu.

Note: Supplementary data for this article are available at Cancer Research Online (http://cancerres.aacrjournals.org/).

Disclosure of Potential Conflicts of Interest
J.W. Tyner reports receiving commercial research grants from Agios, Aptose, Array, AstraZeneca, Constellation, Genentech, Incyte, Janssen, Seattle Genetics, Syros, and Takeda and is a consultant/advisory board member for Leap Oncology. No potential conflicts of interest were disclosed by the other authors.

Authors' Contributions
Conception and design: H. Zhang, J.W. Tyner
Development of methodology: H. Zhang
Acquisition of data (provided animals, acquired and managed patients, provided facilities, etc.): H. Zhang, S. Means, A.R. Schultz, K. Watanabe-Smith, B.C. Medeiros
Analysis and interpretation of data (e.g., statistical analysis, biostatistics, computational analysis): H. Zhang, S. Means, A.R. Schultz, B.C. Medeiros, B. Wilmot, S.K. McWeeney, T. Kükenshöner, O. Hantschel, J.W. Tyner
Writing, review, and/or revision of the manuscript: H. Zhang, A.R. Schultz, K. Watanabe-Smith, B.C. Medeiros, T. Kükenshöner, O. Hantschel, J.W. Tyner
Administrative, technical, or material support (i.e., reporting or organizing data, constructing databases): D. Bottomly
Study supervision: O. Hantschel, J.W. Tyner

disruption of original cysteine pairs in the CSF3R extracellular domain resulted in either gain- or loss-of-function changes, part of which was attributable to cysteine-mediated dimer formation. This, therefore, represents the first characterization of unpaired cysteines that mediate both gain- and loss-of-function phenotypes. Overall, our results show the structural and functional importance of conserved extracellular cysteine pairs in CSF3R and suggest the necessity for broader screening of CSF3R extracellular domain in leukemia patients.

Introduction

G-CSF (also known as CSF3) and its receptor CSF3R play important roles in myelopoiesis, stem cell mobilization, and granulocyte function. CSF3R contains an extracellular, a transmembrane, and a cytoplasmic domain. Similar to other type I cytokine receptor superfamily members, upon ligand binding, CSF3R forms homodimers that bring the cytoplasmic domains into close proximity. This leads to the activation of the JAK–STAT, MAPK/ERK, and PI3K/AKT signaling pathways, which consequently promote cell growth, differentiation, and survival.

Recently, CSF3R mutations have been identified in various hematologic malignancies. CSF3R gain-of-function mutations have two subgroups. The first subgroup is point mutations (T618I, T615A, and T640N) within CSF3R membrane-proximal (exon 14) and transmembrane regions. The majority of these mutations are identified in WHO-defined chronic neutrophilic leukemia (CNL; refs. 1, 2). These missense mutations cause constitutive receptor dimerization, leading to ligand-independent proliferation of myeloid progenitors and inducing a lethal myeloproliferative disorder in a murine bone marrow transplant model (1–4). Another group of CSF3R gain-of-function mutations are truncations (frameshift and stop gain) of CSF3R (T738-Q823), which disrupt the receptor-trafficking pathway, resulting in delayed receptor internalization (5) and/or degradation (6). The resulting CSF3R accumulation induces sustained STAT5 activation and enhanced cell proliferation (6, 7). These truncation mutations are mostly seen in severe congenital neutropenia patients with leukemia transformation or in CNL patients, typically in conjunction with a membrane-proximal mutation (1, 6, 8).

In contrast, the CSF3R loss-of-function mutations identified so far are truncation or missense mutations located in the extracellular domain of CSF3R (9, 10). These mutations are predominantly seen in neutropenia patients. The extracellular region of CSF3R contains an immunoglobulin-like (IgG-like) domain (amino acids 25–117), a cytokine-binding homology region [CHR, also called fibronectin like type III (FNIII) domain 1 and 2, amino acids 117–332], and three other FNIII domains (amino acids 332–623). The IgG-like and CRH domain (especially the WSXWS motif in the CRH domain) mediates the interaction with G-CSF (11). The loss-of-function truncation mutations truncate CSF3R around the WSXWS motif or the transmembrane domain, therefore preventing activation of the cytoplasmic domain (12–14). The loss-of-function missense mutations (e.g., P206H and R308C) are located at or close to the ligand-binding region, which disrupt or abrogate the ligand-binding conformation and lead to G-CSF hyposensitivity or nonresponsiveness (9, 10).

In the current study, we have aimed to identity and characterize novel CSF3R extracellular missense mutations from exome sequencing of leukemia patients.

Materials and Methods

Patient information and study approval

The study was approved by the Institutional Review Boards from Oregon Health & Science University (Portland, OR) and Stanford University School of Medicine (Stanford, CA) and conducted in accordance with guidelines from the Declaration of Helsinki. Written informed consents were obtained from all the patients with Institutional Review Board–approved protocols.

Next-generation sequencing, targeted deep sequencing, and Sanger confirmation

Exome sequencing was performed on a HiSeq 2500 using Illumina Nextera capture probes and paired-end 100-cycle protocols. Targeted deep sequencing was performed using an Ion AmpliSeq custom designed panel. Detailed information is provided in Supplementary Data.

Cell lines and reagents

HEK293T/17 (ATCC, 2006) and NIH/3T3 (ATCC, 2003) cells were maintained in DMEM (Invitrogen) supplemented with 10% FBS (Atlanta Biologicals), L-glutamine, penicillin/streptomycin (Invitrogen), and fungizone (Thermo Fisher Scientific). Ba/F3 cells (ATCC, year unknown) were maintained in RPMI1640 (Invitrogen) supplemented with 10% FBS, 15% WEHI-conditioned media, L-glutamine, penicillin/streptomycin, and fungizone. Low passage cells (<passage 15) were used in the experiments and maintained in *in vitro* culture within 4 weeks. Mycoplasma contamination was tested every other month. Only mycoplasma-free cells were used in the experiments. We did not perform additional authentication test.

Retroviral vector production and transduction

CSF3R mutations were generated using the QuikChange II XL Site-Directed Mutagenesis Kit (Agilent Technologies) on a CSF3R WT pDONR vector (NM_000760.2, GeneCopoeia) and cloned into a gateway compatible MSCV-IRES-GFP retroviral vector via Gateway Cloning System (Invitrogen). Retrovirus was produced by HEK293T/17 cells and transduced into Ba/F3 cells. Transduced Ba/F3 cells with equal intensity of GFP were sorted by flow cytometry (FACS, AriaII, BD Biosciences). For coimmunoprecipitation, a V5-tagged pcDNACSF3R vector (Thermo Fisher Scientific, 12290010) and a modified FLAG-tagged p3xFLAG CMV14 vector were used (3).

TOPO TA cloning

RNA was extracted using RNeasy kits and was reverse transcribed into cDNA using SuperScript VILO II cDNA Synthesis Kit (Thermo Fisher Scientific). The cDNA was then cloned into TOPO TA vector using TOPO TA Cloning Kit (Thermo Fisher Scientific) according to the manufacturer’s protocol and followed by Sanger sequencing with the following primers: forward: 5′-CCTA-CACCCTGCAGATACGC-3′; reverse: 5′-CATCCCATGGACCCG-GATC-3′.

IL3 withdrawal assay

Stably transduced Ba/F3 cells (1×10^6) were washed 3 times and grown in cytokine-free media. Viable cell number was determined on a Guava Personal Cell Analysis System (Millipore) every 1 to 2 days.

FACS analysis

Cells were stained with an anti-CD114 antibody (BioLegend, 346108) for 20 minutes at room temperature and washed twice with PBS. Membrane CSF3R expression was determined by FACS.

Immunoblotting and co-IP

Immunoblotting and co-IP were performed as described previously (3). Briefly, for reducing conditions, 8% β-mercaptoethanol was added into 3× SDS sample buffer [75 mmol/L Tris (pH 6.8), 3% SDS, 15% glycerol, and 0.1% bromophenol blue]. The mixed samples were boiled for 5 minutes in a 95°C heat block before loading on a 4% to 15% Tris-HCl gradient gel (Bio-Rad). For nonreducing conditions, no β-mercaptoethanol was added, and the nonboiled samples were loaded on a 10% gel. The following primary antibodies and reagents were used: anti-GCSF receptor antibody (Abcam, ab126167), anti-GFP antibody (Santa Cruz Biotechnology, sc-9996), anti-pSTAT3 Tyr705 (Cell Signaling Technology, 9131), anti-STAT3 (Cell Signaling Technology, 9132), anti-pSTAT5 Tyr694 (Cell Signaling Technology, 9151), anti-STAT5 (BD Transduction Laboratories, 610192), anti-pERK1/2 Thr202/Tyr204 (Cell Signaling Technology, 4370), anti-ERK1/2 (Cell Signaling Technology, 9102), anti-pJAK2 Tyr1007/1008 (Cell Signaling Technology, 3776), anti-JAK2 (Cell Signaling Technology, 3230), and HRP conjugate secondary antibodies against mouse IgG and rabbit IgG (Promega).

Cell viability assay

Transformed Ba/F3 cells were seeded in 384-well plates (1,250 cells/well) and exposed to increasing concentrations of ruxolitinib, JAK inhibitor I, dasatinib, or imatinib for 72 hours. Cell viability was measured using a methanethiosulfonate (MTS)-based assay (CellTiter96 Aqueous One Solution; Promega) and read at 490 nm after 1 to 3 hours using a BioTek Synergy 2 plate reader (BioTek). Cell viability was determined by comparing the absorbance of drug-treated cells with that of untreated controls set at 100%. IC_{50} values were calculated by regression curve fit analysis using GraphPad Prism software. All drugs were obtained from commercial vendors.

Homology modeling of CSF3R

As there are no crystal structures of CSF3R that contain W341, we built a homology model using SWISS-MODEL (15). The SWISS-MODEL template library (SMTL version 2016-06-29, PDB release 2016-06-24) was searched with Blast and HHBlits for evolutionary-related structures matching the sequence of CSF3R. The highest scoring template for model building was the crystal structure of the extracellular domain of human gp130 (IL6 receptor subunit beta, PDB ID 3L5H) with a sequence identity of 30.3%, which also shares the general domain organization of the class of tall cytokine receptors with one IgG-like C2 domain followed by five FNIII domains. Models are built on the basis of the target-template alignment using ProMod3. Coordinates that are conserved between the target and the template are copied from the template to the model. Insertions and deletions are remodeled using a fragment library. Side chains are then rebuilt. Finally, the geometry of the resulting model is regularized by using a force field. Structural representations of the model are done with PyMOL.

Inhibitor panel screening

Primary patient sample was ficolled, and the isolated peripheral blood mononuclear cells (PBMC) were screened using a panel of small-molecule inhibitors as described previously (16). Briefly, PBMCs were seeded in 384-well plates with a panel of graded concentrations of small-molecule inhibitors and incubated for 72 hours. Cell viabilities were calculated as described in the cell line viability assays.

Statistical analysis

The GraphPad Prism 5 software was used to perform statistical analyses. The data were presented as the mean ± SEM. Statistical significance was determined using Student two-tailed t tests and expressed as P value (*, $P < 0.05$).

Results

Identification of a gain-of-function CSF3R extracellular domain mutation, W341C

We screened 173 CNL/atypical chronic myeloid leukemia (aCML)/unclassified myeloproliferative neoplasm (MPN-U) patients, 199 acute myeloid leukemia (AML), and 106 chronic myeloid leukemia (CML) patients. Four CSF3R extracellular domain missense mutations (P71R, T231M, E288G, and Q346R) were identified in CNL/aCML/MPN-U group and one mutation (W341C) in an AML patient. No CSF3R extracellular mutations were found in a similar CML cohort. We first performed IL3 withdrawal and G-CSF response assays to determine the functional changes of these mutations. We found that W341C transformed Ba/F3 cells to both IL3 and G-CSF–independent growth. In agreement, W341C induced enhanced JAK2, STAT5, and ERK activation compared with the wild-type (WT) receptor (Fig. 1A and B) in transfected HEK293T/17 cells. Alternative mutations at residue W341 (W341A/G/K/R/S) did not result in factor-independent growth (Fig. 1C and D). Similarly, substitutions at other nearby residues, including W342C, W356C, L361C, and W477C, did not show similar leukemogenic potential as W341C (Fig. 1C and D), suggesting that both the cysteine substitution and the amino acid position 341 are essential for this transforming capacity.

Clinical information of the patient harboring the CSF3R W341C/W791X mutation

A 73-year-old female was diagnosed with AML with normal karyotype and negative for NPM1, FLT3-ITD, FLT3 tyrosine kinase domain, and CEBPα mutations. Retrospective exome sequencing later identified a BCOR mutation with 15% variant allelic frequency

(VAF) and a CSF3R truncation mutation W791X with 9.5% VAF (Supplementary Tables S1 and S2). She was enrolled into a clinical trial (ClinicalTrials.gov identifier: NCT01358734) and randomized to the single-agent azacitidine arm (75 mg/m^2, subcutaneous × 7 days every 28 days). Following 8 cycles of therapy, a partial remission was noted (Table 1; Fig. 2). The patient achieved complete morphologic remission with evidence of minimal residual disease observed by FACS after 18 cycles of therapy. The patient was maintained on protocol-defined therapy until cycle #21, at which time, it was observed that the patient's white blood cell (WBC) count (mature neutrophils in particular) progressively increased with an associated downward trend in the patient's platelet count, as well as permanent thrombocytopenia observed at the start of cycle #29. Repeat bone marrow biopsies and aspirations (Table 1) consistently revealed marked marrow hypercellularity with myeloid lineage predominance, but an absence of relapsed AML. Exome and RNA sequencing analyses were negative for BCR-ABL, PDGFRA, PDGFRB, and FGFR1 rearrangement as well as JAK2 mutations. The patient's WBC and absolute neutrophil count constantly rose while progressive thrombocytopenia ensued. Unfortunately, the patient became platelet transfusion dependent by cycle #35 and died of intracranial hemorrhage after 40 cycles on trial, 19 months after the acquisition of a CSF3R compound mutation. Retrospective exome sequence demonstrated the acquisition and expansion of a CSF3R extracellular mutation W341C on the same allele as the CSF3R truncation mutation W791X, which occurred concomitantly with the disease progression (Fig. 2; Supplementary Fig. S1; Supplementary Table S2).

W341C induces intermolecular disulfide bond formation and leads to increased receptor dimerization

Point mutations that insert a cysteine into the extracellular domain of multiple receptors (IL7R, CRLF2, RET, and EpoR; refs. 17–21) have been previously shown to confer oncogenic potential by inducing disulfide bond–mediated dimerization. To test the possibility that this same mechanism was eliciting transforming capacity by CSF3R W341C, we first quantified dimer formation induced by this mutation. Indeed, we observed markedly increased dimerization of the mutant protein compared with WT in co-IP assays and in immunoblots under nonreducing conditions, which was abrogated in a reducing condition immunoblot (Fig. 3A–C). In contract, as shown in Fig. 3C, other W341 substitutions (W341A/G/K/R/S), W342C, L361C, and W477C demonstrated similar subtle dimerization as WT. Surprisingly, the W356C substitution, which showed a loss-of-function phenotype, demonstrated increased dimerization similar to W341C, suggesting that increased receptor dimerization alone is not sufficient for the transforming potential.

Structural modeling of W341

We next attempted to map the structural location of this variant in hopes of informing mechanistic understanding of why the W341C mutation is transforming. Available crystal structures of CSF3R are restricted to its N-terminal Ig-like C2 and CHR domain, which form the binding site for G-CSF (11). These constructs end around residue 300 and, therefore, do not contain the W341 and W356 residues. Hence, we built a homology model of the entire extracellular domain of CSF3R based on the crystal structure of the entire extracellular domain of gp130 (22), which is the structure with the highest sequence homology to CSF3R.

Importantly, CSF3R and gp130 have the same domain organization and both belong to the family of tall cytokine receptors. In the model, the third and fourth FNIII domains make an extensive intramolecular domain–domain interface that orients these two domains almost perpendicular to each other. Excitingly, W341, located in the third FNIII domain, is positioned in the center of this interface and binds a hydrophobic cavity in the fourth FNIII domain. On the basis of this central location, it is very likely that the W341C mutation will perturb the largely hydrophobic interaction interface of the third and fourth FNIII domain. As a consequence, changes in the overall domain arrangement of CSF3R are likely. This could either favor a conformation that results in ligand-independent activation of the receptor, or the introduced cysteine residue may become exposed to form inter- or intra-molecular disulfide bonds to activate CSF3R. In line with this, we observed increased dimers in the W341C protein. It is therefore conceivable that W341C forms intermolecular disulfide bonds. Interestingly, computational modeling analysis indicated that the side chains of W341 and W356 point in opposite directions, which might be a possible explanation for the differing functional consequences of the W356C and W341C mutations. On the basis of our functional data, we propose that W341C-mediated intermolecular disulfide bond forms active dimers that may orientate the phosphorylation sites of the cytoplasmic domain to be in close proximity, thereby resulting in transactivation and initiation of downstream signaling. In contrast, W356C could form inactive dimers that may place the phosphorylation sites at a distance from each other, thereby eliminating the opportunity for transactivation, even in the presence of G-CSF (Fig. 3D).

Interestingly, R308C was previously shown to be a loss-of-function mutation, and the functional change was attributed to disrupting the cation–π stacking interaction located close to the WSWX motif (10). However, we observed increased dimer and loss-of-function phenotype of R308C, but not R308S (Supplementary Fig. S2), suggesting that, similar to W356C, disulfide bond–mediated inactive dimers may also play a role in the loss-of-function phenotype of R308C.

CSF3R W341C/W791X compound mutation demonstrates enhanced oncogenic potential

On the basis of the variant allele fraction, the CSF3R W341C mutation was a heterozygous mutation with 38.4% allelic burden. Interestingly, the CSF3R truncation mutation W791X was present with 50% allelic burden (Fig. 2; Supplementary Table S2). We sequenced cDNA material from the patient and found that W341C and W791X were on the same allele. Therefore, we studied the biological consequences of the W341C/W791X compound mutation. W341C/W791X demonstrated increased protein, resulting in increased dimers compared with WT and transformed Ba/F3 with faster kinetics compared with W341C alone (Fig. 4A and B). As CSF3R cytoplasmic truncation mutations, including W791X, were shown to interrupt receptor degradation (6), we quantified the total receptor via immunoblot after a time course of cycloheximide treatment. Markedly reduced receptor degradation of W341C/W791X, but not the single mutation or WT, was observed (Fig. 4C; Supplementary Fig. S3). Furthermore, both W341C and W341C/W791X–transformed cells were sensitive to ruxolitinib and JAK inhibitor I (Fig. 4D). Notably, primary cells from the patient harboring this mutation demonstrated sensitivity to JAK inhibition (Fig. 4E).

Disruption of the intramolecular cysteine pairs demonstrates either gain- or loss-of-function phenotypes

Sarabipour and colleagues showed that disruption of the intramolecular cysteine pairs of FGFR (FGFR1 C178S, FGFR2 C342R, and FGFR3 C228R) created unpaired cysteines and led to constitutive receptor activation via intermolecular disulfide bond–mediated dimerization (23). Accordingly, we postulated that disruption of the cysteine pairs in the CSF3R extracellular domain may demonstrate a similar gain-of-function phenotype. There are five characterized cysteine pairs (11) and potentially one additional cysteine pair within the CSF3R extracellular domain (Supplementary Fig. S4). We generated CSF3R missense mutations disrupting these cysteine pairs. Interestingly, these mutations demonstrated the loss of the upper CSF3R band and reduced receptor surface expression (Fig. 5A and B), suggesting that cysteine-mediated disulfide bonds play important roles for the receptor maturation and surface expression. Interestingly, we observed either gain (C177Y, C248A, and C309Y) or loss (C131Y, C167Y, C186Y, C266Y, C295A, and C388Y)-of-function changes (Fig. 5C and D). Interestingly, the gain-of-function mutations C248A and C309Y formed increased disulfide bond–mediated dimers, whereas C177Y did not change the dimer formation (Fig. 5A). In addition, C177Y demonstrated G-CSF hypersensitivity (Fig. 5D). Surprisingly, similar to W356C, the loss-of-function mutations at C266Y, C295A, and C388Y also formed increased disulfide bond–mediated dimers, whereas C131Y, C167Y, and C186Y did not alter dimer formation (Fig. 5A). We performed computing modeling of these cysteine mutations (Fig. 5E); however, we did not find a correlation between cysteine positions and functional consequences.

Double cysteine mutations abrogate the gain-of-function phenotype and part of the loss-of-function phenotype

We further examined whether impaired intramolecular disulfide bonding, *de novo* formation of intermolecular disulfide bonds, or both are essential for the phenotypic and functional changes in mutations with increased dimer formation. C248 and C295 are paired cysteines; however, C248A and C295A mediated gain- and loss-of-function changes, respectively, indicating that *de novo* formation of intermolecular disulfide bonds may be required for the functional changes. In agreement, double mutation at C248A/C295A abrogated the gain-of-function and increased dimer formation seen with the C248A single mutation, indicating the unpaired C295 and the disulfide bond–mediated dimer are essential for the gain of function in C248A (Supplementary Fig. S5). In addition, C266Y and C309Y are paired cysteines; however, they also mediated opposite functional changes. In concordance with the C248/C295 data, double mutation at C266Y/C309Y also reduced the dimer levels seen with the single mutations, C266Y and C309Y, and abrogated the gain of function of the single mutation C309Y. These results indicate that disruption of an intramolecular disulfide bond is essential for the gain-of-function change of C309Y. On the contrary, double mutation C266Y/C309Y also mediated a loss-of-function phenotype, indicating the *de novo* formation of intermolecular bonds induced by the C266Y mutation is not absolutely required for the loss-of-function change of C266Y (Supplementary Fig. S5A and S5B). However, C388Y/C395Y demonstrated similar dimer expression and G-CSF response, indicating that the loss of function change of C388Y occurred in a *de novo* disulfide bond–dependent manner (Supplementary Fig. S5B and S5C).

Discussion

Here, we described the identification of a novel gain-of-function mutation, W341C, in the extracellular domain of CSF3R in a leukemia patient. This mutation, which was observed together with a truncation mutation, W791X, on the same allele, was associated with progressive leukocytosis and thrombocytopenia of this patient. *In vitro* studies showed that W341C induced constitutive activation of downstream JAK/STAT and ERK activation, causing G-CSF–independent cell growth and transformation of Ba/F3 cells (Figs. 1 and 2). In addition, the compound mutation demonstrated enhanced oncogenic potential (Fig. 3).

We further characterized that the oncogenic mechanism of W341C is associated with unpaired cysteine-mediated disulfide bond formation, leading to dimer stabilization (Fig. 3). Homology modeling indicated that the amino acid 341 is located at a position with the FLexibility to form a disulfide bond, whereas L361 and W477 are located at positions less likely to form disulfide bonds. Surprisingly, we also observed that W356C, which abrogated receptor surface expression and G-CSF response, demonstrated disulfide bond–mediated increases in receptor dimerization, similar to W341C. Computational modeling analysis indicated that the side chains of W341 and W356 point in opposite directions, which may mediate active and inactive dimers, respectively, as proposed in our model (Fig. 3C).

In addition, and in light of previous findings (23), we propose that mutations disrupting the original cysteine pairs may also confer oncogenic potential via intermolecular disulfide bond formation. Surprisingly, we observed two opposite functional consequences: gain (C177Y, C248A, and C309Y) and loss (C137Y, C167Y, C266Y, and C388Y) of function when disrupting CSF3R extracellular cysteine pairs. We did not find correlation in terms of the positions of the cysteines with functional consequences. Two of the three gain-of-function mutations, C248A and C309Y, demonstrated increased dimer formation, which was shown further to be imperative for the gain-of-function change (mutating the other paired cysteine abrogated the gain of function phenotype). However, we did not observe increased dimers in C177Y. In addition to cysteine-mediated dimer formation, altering receptor-ligand binding is another common mechanism of extracellular domain mutation-mediated receptor activation, such as gp130 extracellular mutations seen in inflammatory hepatocellular tumors (24). C177 is located in the ligand-binding domain and mediated G-CSF hypersensitivity (Fig. 5D), suggesting that the conformational change induced by C177Y may mimic the effect of ligand binding to the normal receptor, and the further ligand binding may further favor this conformation.

Interestingly, the disulfide bond–mediated dimer is not absolutely required for loss-of-function mutation phenotype (no increased dimer shown in C131Y and C186Y; double mutation C266Y/C309Y demonstrated loss-of-function change; Supplementary Fig. S5), indicating again that the original extracellular cysteine pairs are imperative for the receptor expression and function. In contrast, cysteine-mediated disulfide bonds are required for the loss of function in C295A, C388Y, and R308C (Supplementary Figs. S2 and S5), indicating the *de novo* formation of inactive dimers is indispensable for the loss-of-function change of these mutants.

In conclusion, our study has demonstrated the importance of cysteine-mediated intramolecular disulfide bonds for the normal receptor membrane targeting and ligand receptor response of CSF3R. Furthermore, the study showed multiple pathogenic consequences of cysteine mutations in CSF3R extracellular domain. Briefly, mutations inserting additional cysteines or disrupting the conserved cysteine pairs of CSF3R induce either gain-or loss-of-function changes. Cysteine-mediated gain of function has been characterized in several receptors (IL7R, CRLF2, and FGFR; refs. 20, 21, 23, 25), whereas cysteine-mediated loss of function is less recognized. Our study provides insight and brings attention for further analysis of dual functional changes in cysteine mutation–mediated changes of cytokine/growth factor receptor function.

Genetic screening for CSF3R membrane-proximal, transmembrane, and cytoplasmic domain mutations has increasingly been applied in clinical sequencing panels for leukemia patients. Our results would suggest added value from extending this screening to a broader range of the CSF3R extracellular domain. Finally, given the rapidly progressive neutrophilia and lethal thrombocytopenia observed in the index patient reported here, other patients with extracellular CSF3R-activating mutations may benefit from intervention with JAK inhibitor therapy.

Supplementary Material

Refer to Web version on PubMed Central for supplementary material.

Acknowledgments

The authors acknowledge Angela Rofelty and Samantha Savage for preparation of the DNA and RNA sequence samples. The authors thank Cristina Tognon and Corinne Visser for collecting the patient’s data, Dorian LaTocha and Brianna Garcia for help in the FACS sorting, Samantha Savage for the instruction of targeted deep sequencing, and Marilynn Chow, Tamilla Nechiporuk, and Kara Johnson for general help.

Grant Support

J.W. Tyner was supported by The Leukemia & Lymphoma Society, the V Foundation for Cancer Research, the Gabrielle’s Angel Foundation for Cancer Research, and the NCI (5R00CA151457-04 and 1R01CA183947-01). O. Hantschel and T. Kükenshöner are supported by Swiss National Centre of Competence in Research-Chemical Biology.

References

1. Maxson JE, Gotlib J, Pollyea DA, Fleischman AG, Agarwal A, Eide CA, et al. Oncogenic CSF3R mutations in chronic neutrophilic leukemia and atypical CML. N Engl J Med. 2013; 368:1781–90. [PubMed: 23656643]
2. Maxson JE, Luty SB, MacManiman JD, Paik JC, Gotlib J, Greenberg P, et al. The Colony Stimulating Factor 3 Receptor T640N mutation is oncogenic, sensitive to JAK inhibition, and mimics T618I. Clin Cancer Res. 2015; 22:757–64. [PubMed: 26475333]
3. Maxson JE, Luty SB, MacManiman JD, Abel ML, Druker BJ, Tyner JW. Ligand independence of the T618I mutation in the colony-stimulating factor 3 receptor (CSF3R) protein results from loss of O-linked glyco-sylation and increased receptor dimerization. J Biol Chem. 2014; 289:5820–7. [PubMed: 24403076]
4. Fleischman AG, Maxson JE, Luty SB, Agarwal A, Royer LR, Abel ML, et al. The CSF3R T618I mutation causes a lethal neutrophilic neoplasia in Mice that is responsive to therapeutic JAK inhibition. Blood. 2013; 122:3628–31. [PubMed: 24081659]

5. Aarts LHJ, Roovers O, Ward AC, Touw IP. Receptor activation and 2 distinct COOH-terminal motifs control G-CSF receptor distribution and internalization kinetics. Blood. 2004; 103:571–9. [PubMed: 14512302]
6. Zhang H, Reister Schultz A, Luty S, Rofelty A, Su Y, Means S, et al. Characterization of the leukemogenic potential of distal cytoplasmic CSF3R truncation and missense mutations. Leukemia. 2017 May 12. [Epub ahead of print].
7. Liu F, Kunter G, Krem MM, Eades WC, Cain JA, Tomasson MH, et al. Csf3r mutations in mice confer a strong clonal HSC advantage via activation of Stat5. J Clin Invest. 2008; 118:946–55. [PubMed: 18292815]
8. Ward AC, van Aesch YM, Schelen AM, Touw IP. Defective internalization and sustained activation of truncated granulocyte colony-stimulating factor receptor found in severe congenital neutropenia/ acute myeloid leukemia. Blood. 1999; 93:447–58. [PubMed: 9885206]
9. Ward AC, Gits J, Majeed F, Aprikyan AA, Lewis RS, O'Sullivan LA, et al. Functional interaction between mutations in the granulocyte colony-stimulating factor receptor in severe congenital neutropenia. Br J Haematol. 2008; 142:653–6. [PubMed: 18513286]
10. Triot A, Järvinen PM, Arostegui JI, Murugan D, Kohistani N, Díaz JLD, et al. Inherited biallelic CSF3R mutations in severe congenital neutropenia. Blood. 2014; 123:3811–7. [PubMed: 24753537]
11. Tamada T, Honjo E, Maeda Y, Okamoto T, Ishibashi M, Tokunaga M, et al. Homodimeric cross-over structure of the human granulocyte colony-stimulating factor (GCSF) receptor signaling complex. Proc Natl Acad Sci U S A. 2006; 103:3135–40. [PubMed: 16492764]
12. Papadaki HA, Kosteas T, Gemetzi C, Damianaki A, Anagnou NP, Eliopoulos GD. Acute myeloid/NK precursor cell leukemia with trisomy 4 and a novel point mutation in the extracellular domain of the G-CSF receptor in a patient with chronic idiopathic neutropenia. Ann Hematol. 2004; 83:345–8. [PubMed: 15014900]
13. Druhan LJ, Ai J, Massullo P, Kindwall-Keller T, Ranalli MA, Avalos BR. Novel mechanism of G-CSF refractoriness in patients with severe congenital neutropenia. Blood. 2005; 105:584–91. [PubMed: 15353486]
14. Sinha S, Zhu QS, Romero G, Corey SJ. Deletional mutation of the external domain of the human granulocyte colony-stimulating factor receptor in a patient with severe chronic neutropenia refractory to granulocyte colony-stimulating factor. J Pediatr Hematol Oncol. 2003; 25:791–6. [PubMed: 14528102]
15. Arnold K, Bordoli L, Kopp J, Schwede T. The SWISS-MODEL workspace: a web-based environment for protein structure homology modelling. Bio-informatics. 2006; 22:195–201.
16. Tyner JW, Yang WF, Bankhead A, Fan G, Fletcher LB, Bryant J, et al. Kinase pathway dependence in primary human leukemias determined by rapid inhibitor screening. Cancer Res. 2013; 73:285–96. [PubMed: 23087056]
17. Watowich SS. Activation of erythropoietin signaling by receptor dimerization. Int J Biochem Cell Biol. 1999; 31:1075–88. [PubMed: 10582340]
18. Pharr PN, Hankins D, Hofbauer A, Lodish HF, Longmore GD. Expression of a constitutively active erythropoietin receptor in primary hematopoietic progenitors abrogates erythropoietin dependence and enhances erythroid colony-forming unit, erythroid burst-forming unit, and granulocyte/ macrophage progenitor growth. Proc Natl Acad Sci U S A. 1993; 90:938–42. [PubMed: 7679218]
19. Arlt DH, Baur B, Wagner B, Höppner W. A novel type of mutation in the cysteine rich domain of the RET receptor causes ligand independent activation. Oncogene. 2000; 19:3445–8. [PubMed: 10918602]
20. Yoda A, Yoda Y, Chiaretti S, Bar-Natan M, Mani K, Rodig SJ, et al. Functional screening identifies CRLF2 in precursor B-cell acute lymphoblastic leukemia. Proc Natl Acad Sci U S A. 2010; 107:252–7. [PubMed: 20018760]
21. Shochat C, Tal N, Bandapalli OR, Palmi C, Ganmore I, te Kronnie G, et al. Gain-of-function mutations in interleukin-7 receptor-α (IL7R) in childhood acute lymphoblastic leukemias. J Exp Med. 2011; 208:901–8. [PubMed: 21536738]

22. Xu Y, Kershaw NJ, Luo CS, Soo P, Pocock MJ, Czabotar PE, et al. Crystal structure of the entire ectodomain of gp130: insights into the molecular assembly of the tall cytokine receptor complexes. J Biol Chem. 2010; 285:21214–8. [PubMed: 20489211]
23. Sarabipour S, Hristova K. Pathogenic cysteine removal mutations in FGFR extracellular domains stabilize receptor dimers and perturb the TM dimer structure. J Mol Biol. 2016; 428:3903–10. [PubMed: 27596331]
24. Rebouissou S, Amessou M, Couchy G, Poussin K, Imbeaud S, Pilati C, et al. Frequent in-frame somatic deletions activate gp130 in inflammatory hepatocellular tumours. Nature. 2009; 457:200–4. [PubMed: 19020503]
25. Shochat C, Tal N, Gryshkova V, Birger Y, Bandapalli OR, Cazzaniga G, et al. Novel activating mutations lacking cysteine in type i cytokine receptors in acute lymphoblastic leukemia. Blood. 2014; 124:106–10. [PubMed: 24787007]

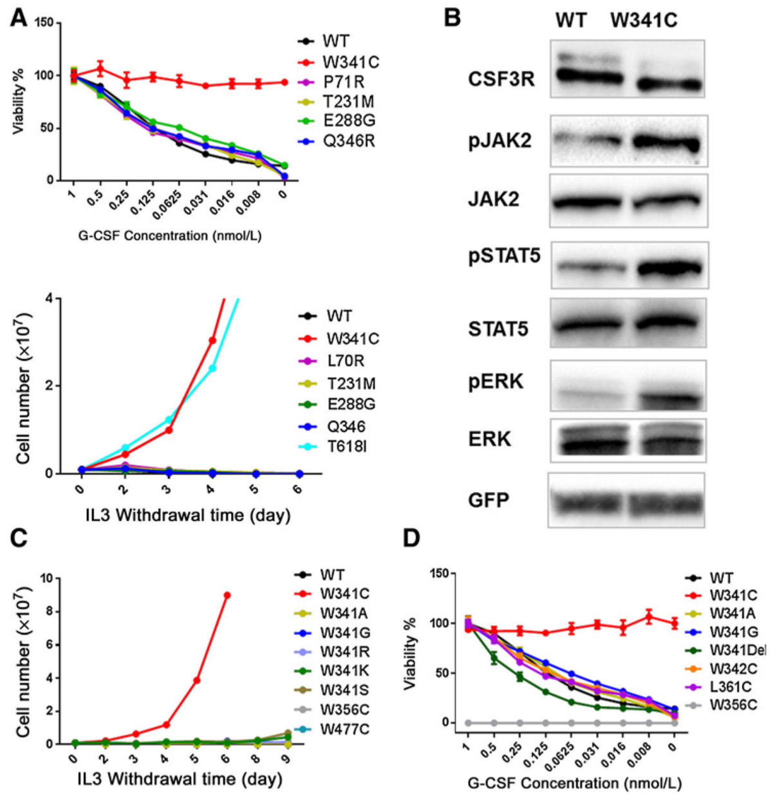

Figure 1. Identification of a CSF3R extracellular autoactivating mutation W341C

A, Top, Ba/F3 cells expressing CSF3R WT and mutants were plated with a concentration gradient of G-CSF after removing IL3 and cultured for 72 hours and subjected to MTS assay.

Representative graph depicts percentage of cell viability (mean ± SEM) normalized to the highest G-CSF concentration (1 ng/mL) for each cell line. Bottom, representative IL3 withdrawal assay of Ba/F3 cells expressing CSF3R WT and extracellular mutations. T618I cells were used as a positive control.

B, HEK293T/17 cells were transfected with CSF3R WT and W341C constructs for 48 hours. Transfected cells were then serum starved for 4 hours and subjected to immunoblot probing for CSF3R, pJAK2, pSTAT5, and pERK.

C, Representative transforming assay of Ba/F3 cells expressing tryptophan to cysteine substitution at different amino acid positions and tryptophan to other amino acid substitutions at 341. **D,** Ba/F3 cells expressing CSF3R WT and mutants were plated with a concentration gradient of G-CSF after removing IL3 and cultured for 72 hours and subjected to MTS assay.

Representative graph depicts percentage of cell viabilities (mean ± SEM) normalized to the highest G-CSF concentration (1 ng/mL) for each cell line. Images shown are representative of at least three independent experiments.

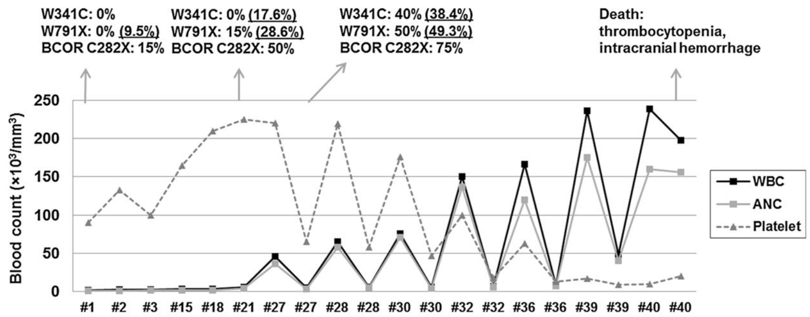

Figure 2.

W341C/W791X causes progressively increased WBC and absolute neutrophil count of the patient. Serial WBC, platelet, and absolute neutrophil counts with mutation status during treatment. BCOR mutation was validated with Sanger sequencing. Mutations of CSF3R were validated with Sanger sequencing and targeted deep sequencing (highlighted with underline).

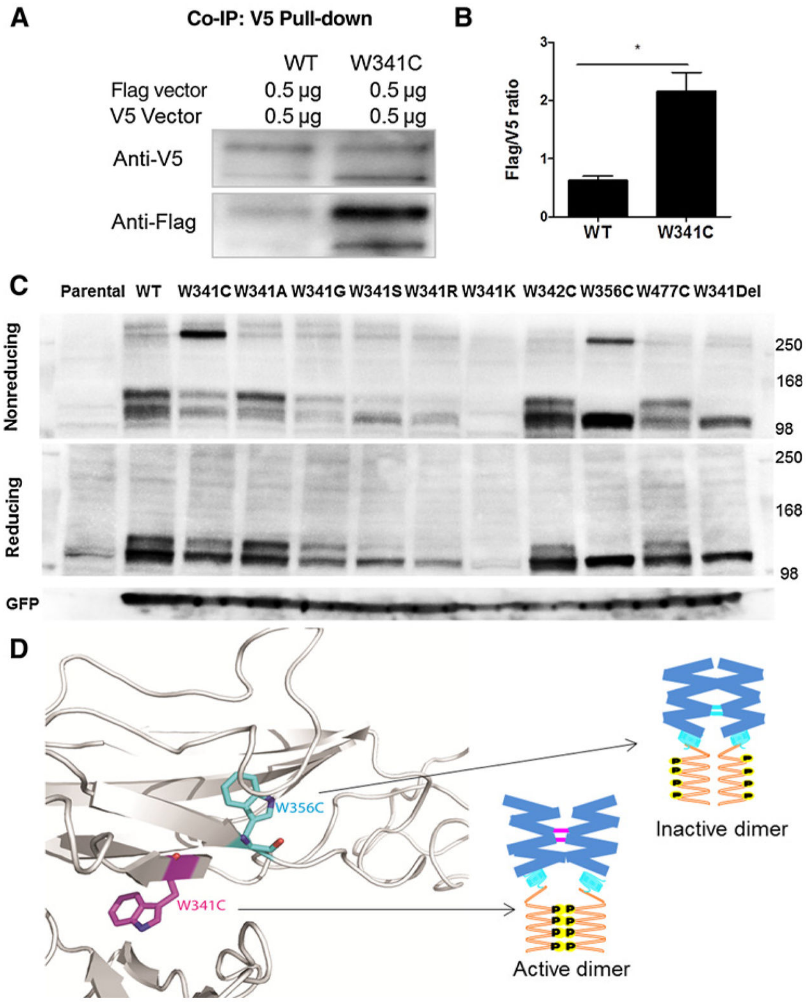

Figure 3. W341C induces intermolecular disulfide bond formation and leads to increased receptor dimerization

A, HEK293T/17 cells were transfected with equal amount of Flag- and V5-tagged CSF3R WT or W341C construct for 48 hours and subjected to co-IP assay. Representative immunoblot image demonstrates increased CSF3R pull-down in W341C cells. **B,** Graph depicts increased Flag/V5 ratios of CSF3R W341C compared with WT in co-IP assay of three independent experiments. Data, mean ± SEM. Statistical significance was determined using Student two-tailed *t* tests and expressed as *P* value (*, $P < 0.05$). **C,** CSF3R expression determined by nonreducing (top) and reducing immunoblots (bottom) in transfected HEK293T/17 cells expressing CSF3R variants. Protein molecular weight markers are shown on both sides. Images shown are representative of more than three independent experiments. **D,** Homology model of the CSF3R extracellular domain. W341 and W356 are shown in stick representation. A hypothesized model involving active and inactive dimer is illustrated.

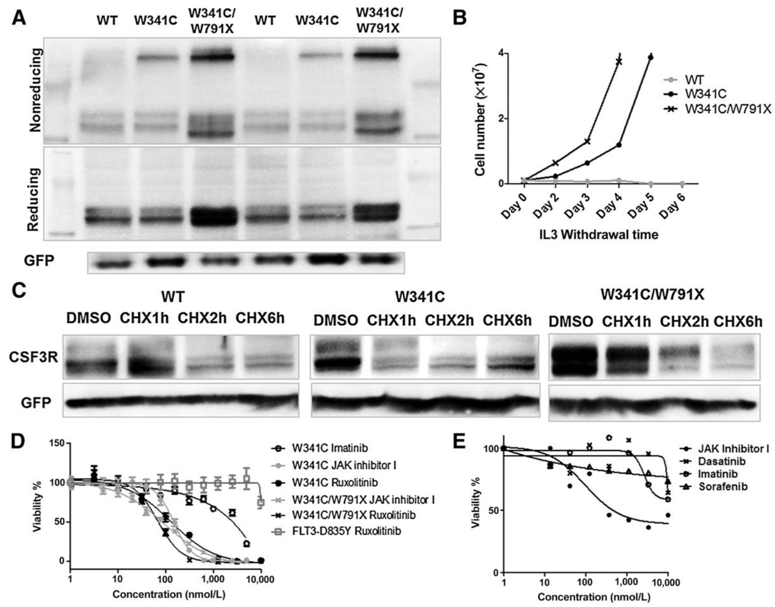

Figure 4.
The CSF3R W341C/W791X compound mutation demonstrates enhanced oncogenic potential. **A,** Representative immunoblot image of CSF3R expression of WT, W341C, and W341C/W791X compound mutation in nonreducing and reducing conditions. Protein molecular weight marker was shown on both sides. **B,** Representative IL3 withdrawal assay demonstrated faster outgrowth kinetics of Ba/F3 cells expressing the W341C/W791X compound mutation compared with W341C alone. **C,** Representative immunoblot images showing CSF3R expression in HEK293T/17 cells transiently transfected with WT, W341C, or W341C/W791X after cycloheximide (CHX; 100 mg/mL) treatment. **D,** Transduced Ba/F3 cells were treated with gradient concentrations of different inhibitors for 72 hours, and cell viability was assessed by MTS assay as described in Materials and Methods. Graph depicts percentages of cell viability (mean ± SEM) at different drug concentrations normalized to nondrug treatment control. Images shown are representative of at least three independent experiments. FLT3-D835Y–transformed Ba/F3 cells were used as control. **E,** Primary patient PBMCs were plated with graded concentrations of a panel of small-molecule inhibitors for 72 hours, and cell viability was determined by MTS assay. Graph depicts percentages of cell viability of different inhibitors at different drug concentrations normalized to nondrug treatment control.

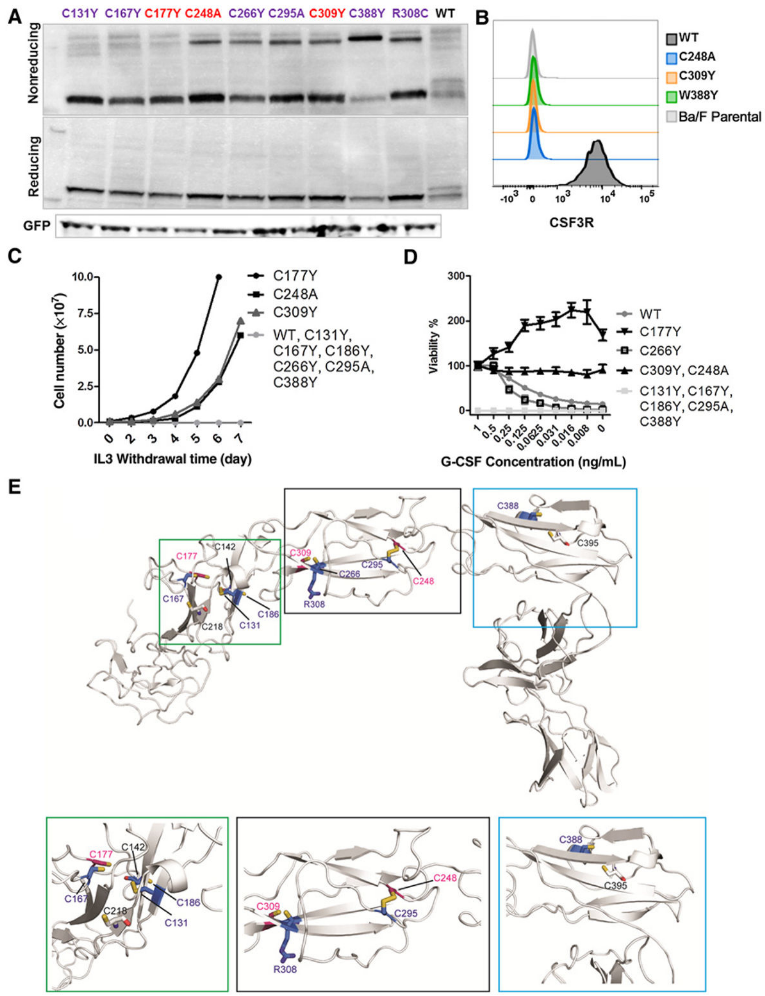

Figure 5.

Disruption of the intramolecular cysteine pairs demonstrates either gain- or loss-of-function phenotypes. **A,** CSF3R expression determined by nonreducing (top) and reducing (bottom) immunoblots in transfected HEK293T/17 cells. Protein molecular weight marker is shown on the left side. Images shown are representative of three independent experiments. **B,** Representative histogram depicts surface CSF3R expression. **C,** Representative IL3 withdrawal assay of Ba/F3 cells expressing mutations disrupting the cysteine pairs at the CSF3R extracellular domain. **D,** Ba/F3 cells expressing CSF3R WT and mutants were plated with a concentration gradient of G-CSF after removing IL3 and cultured for 72 hours and subjected to MTS assay. **E,** Homology models the CSF3R extracellular domain. The structural location of the mutants of extracellular cysteine pairs is shown in stick representation and is colored according to their phenotype after substitution of cysteine (violet, loss of function; red, gain of function; black, uncharacterized).

Table 1

Serial blood counts of peripheral blood and bone marrow aspiration of the patient carrying W341C/W791X at diagnosis and during treatment

Time point	PB WBC ($\times 10^3/mm^3$)	PB ANC ($\times 10^3/mm^3$)	PB blasts	PB platelets	BM blasts	BM cellularity
#1	1.7	0.68	0	90	23%	40%
#5	2.5	1.2	0	132	10%	60%
#8	2.5	1.56	0	150	6%	50%
#18	5.6	4.32	0	225	0%	60%
#21	16.3	13.7	0	209	1%	60%
#27	75.4	70.8	2%	176	2%	90%
#36	156.5	114.2	1%	44	3%	100%

Abbreviations: ANC, absolute neutrophil count; BM, bone marrow; PB, peripheral blood; WBC, white blood cell count.